Alkali Corrosion-Resistant Heat Insulation Materials

N. Brachhold, Chr. G. Aneziris

Alkali corrosion in high temperature furnaces is an increasing problem due to the use of secondary fuels, such as waste material and biomass. They contain higher amounts of alkali components than conventional energy carriers and enhance corrosion reactions. This study investigated a new approach based on alkali aluminosilicates which are typical corrosion products of fire clay related heat insulation materials. In the synthesis experiments, three processing routines were investigated: a hydrothermal treatment up to temperatures of 200 °C, a thermal treatment up to temperatures of 1200 °C and a combination of both technics. The phase composition and the alkali corrosion behaviour of the synthesized materials were investigated. The analysis showed that the relation between phase composition and the corrosion behaviour of the synthesized materials were complex. The stoichiometry of $KAlSiO_4$ yielded a promising material. An appropriate shaping technology was established. The resulting shaped samples were basically characterized with regard to bulk density, porosity, cold crushing strength, thermal conductivity, refractoriness under load. After testing the material under alkali load on a laboratory scale, the material was successfully applied in the heat insulation lining in an industrial furnace.

1 Introduction

Alkali corrosion is a severe problem in high temperature furnaces because aggressive alkali compounds are constantly introduced by the used raw materials and energy carriers [1–3]. Different corrosion mechanisms are possible [4, 5]. On the one hand, melts can form due to eutectic points, which exist at relatively low temperatures if the furnace lining is in contact with alkali compounds. On the other hand, alkali spalling can be observed if the furnace lining and alkalis react and form alkali containing reaction products. These new phases generally have lower densities in comparison with the initial material what causes the spalling effects. Both effects result in a continuous degradation of the furnace lining. Furthermore, the material loss of the lining as a result of the corrosion processes reduces the lining thickness successively which is accompanied by increasing thermal losses with the advancing corrosion processes. The corrosion effects are intensified if so-called secondary fuels are used as energy carriers [6, 7]. These are all kinds of alternative combustible materials such as biomass, waste materials and tyres. Secondary fuels contain higher amounts of alkalis and additionally chlorine and sulphur containing compounds than conventional fuels. The use of secondary fuels is especially relevant in the cement industry. Therefore, this study presents a new material concept for the heat insulation part of the furnace lining in cement kilns followed by its verification, development of an appropriate process technology and test application in an industrial furnace. This work concentrated on alkali corrosion resistant heat insulation materials based on corrosion products which have been observed in cement kilns [8]. The presence of these phases in the highly corrosive atmosphere indicated that such phases might be stable under such aggressive conditions. Hence, it was postulated that materials based on these compounds should have a prolonged lifetime in alkali containing atmospheres and, therefore, enhance the lifetime cycles of the cement furnace. The synthesis experiments focused on ternary alkali aluminosilicates which are generally observed as corrosion products of fireclay based heat insulation materials with alkalis, namely orthoclase/sanidine/microcline ($KAlSi_3O_8$, abbrev.: KAS_6), leucite ($KAlSi_2O_6$, abbrev.: KAS_4), kaliophilite/kalsilite/orthorhombic $KAlSiO_4$ ($KAlSiO_4$, abbrev: KAS_2), albite ($NaAlSi_3O_8$, abbrev: NAS_6) and carnegieite/nepheline ($NaAlSiO_4$, abbrev.: NAS_2). Furthermore, shaping experiments were undertaken to produce shaped samples for a basic characterisation of the material.

Nora Brachhold, Christos G. Aneziris
Institute of Ceramic, Glass and Construction Material Technology
TU Bergakademie Freiberg
09599 Freiberg
Germany

Corresponding author: *N. Brachhold*
E-mail: nora.brachhold@ikgb.tu-freiberg.de

Keywords: alkali corrosion, alkali aluminosilicates, heat insulation material, cement industry

Received: 05.05.2016
Accepted: 28.09.2016

Tab. 1 Oxidic composition of the investigated target compositions and corresponding batch formulae based on kaolin 1 [10]

Target Compound	Oxidic Composition [mass-%]				Raw Materials [mass-%]				
	K_2O	Na_2O	Al_2O_3	SiO_2	KOH	NaOH	Kaolin	Quartz	$Al(OH)_3$
KAS_6	16,9		18,4	64,7	17,3		53,2	29,6	
KAS_4	21,6		23,4	55,0	12,6		66,0	21,4	
KAS_2	29,8		32,3	40,0	28,5		58,2		13,3
NAS_6		11,8	19,5	68,7		13,3	55,1	31,5	
NAS_2		21,8	35,9	42,3		22,6	63,0		14,4

Tab. 2 Chemical composition of the used kaolins

Kaolin	Oxidic Composition [mass-%]							
	SiO_2	Al_2O_3	Fe_2O_3	TiO_2	CaO	MgO	K_2O	L.o.I.
1	54,0	31,0	0,7	0,3	0,6	0,4	1,3	11,4
2	54,2	32,5	0,38	0,16	0,18	0,25	0,28	11,8

2 Experimental procedure

The oxidic composition of the investigated compounds is shown in Tab. 1, which also presents the used batch formulae. The main raw material was kaolin. Being a natural raw material, it is a relatively low cost source of SiO_2 and Al_2O_3.

Two types of kaolin were used during this investigation: kaolin 1 from VEB Silikatrohstoffkombinat Kemmlitz/DE (former GDR), type Salzmünde and kaolin 2 from AKW Amberger Kaolinwerke, Hirschau/DE type BZ. Their composition is shown in Tab. 2. Kaolin 1 was used for the synthesis investigations. Kaolin 2 was applied for the shaping experiments due to better availability. Additionally, quartz powder SH 300 (Quarzwerke Frechen/DE) or aluminium hydroxide TG7 (TOR Minerals, Corpus Christi, TX/US) were used to realize the intended stoichiometry.

The alkali component was introduced in the system as aqueous solutions of potassium hydroxide (Brenntag AG/DE) or sodium hydroxide (Merck AG/DE). The aqueous solutions were prepared from 50 mass-% of solid alkali hydroxide and 50 mass-% distilled water.

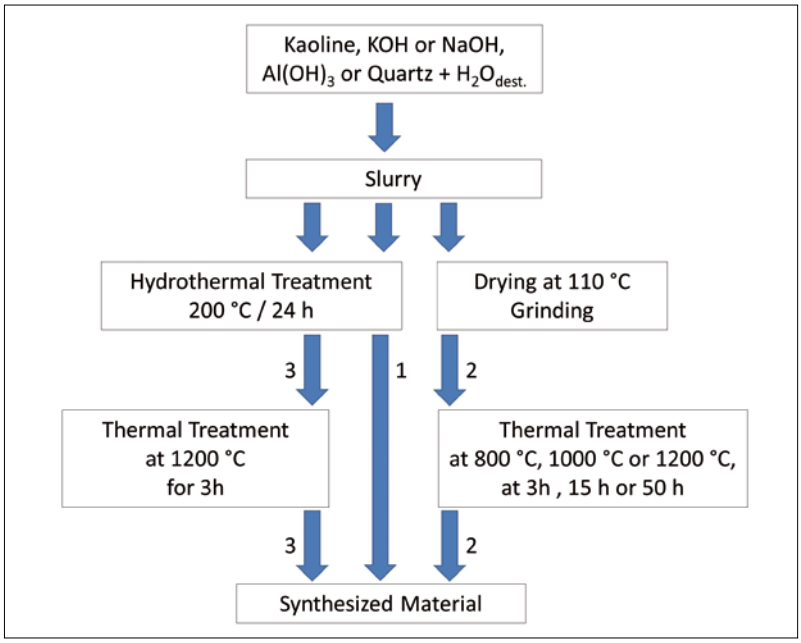

Fig. 1 Schematic representation of the investigated synthesizing routines: 1 – hydrothermal routine, 2 – thermal routine, 3 – combined routine (after [9])

During the synthesizing experiments, three processing routines were investigated (Fig. 1): a hydrothermal routine (200 °C, dwell time 24 h), a thermal routine (synthesis temperature of 800 °C, 1000 °C and 1200 °C, dwell time 3 h, 15 h, 50 h) and the combined routine consisting of the hydrothermal followed by a thermal treatment. The hydrothermal treatment took place in a 50 l-autoclave (Heckmann/DE). For the thermal processing steps, an electric chamber furnace of type N20/14 (Nabertherm/DE) was used.

For each stoichiometry, the raw materials were transferred to a slurry for homogenization purposes. The slurry was directly used for the hydrothermal treatment of processing routines 1 and 3. For the synthesis via the thermal processing routine, the slurry was dried again, ground to a grain size <1 mm and uniaxially pressed to cylindrical samples (Ø ca. 50 mm, height ca. 10 mm) at 50 MPa (press type ES, Rucks Maschinenbau GmbH/DE) before the thermal treatment.

After the synthesis, the phase composition of the synthesized material was characterized by powder diffractometry (MPD 3040/, PANalytical, Almelo/NL) with CuKα radiation scanning 2θ region from 5° to 90°, using the software X'Pert Highscore Plus (PANalytical, Almelo/NL).

The resulting synthesized material was tested on alkali corrosion by simulation the alkali attack using a mixture of alkali salts. The testing procedure was presented in detail in a previous study [7, 8]. The salt mixture (K_2SO_4 : K_2CO_3 : KCl = 1 : 1 : 1 by weight) is added to the ground material to be tested in the ratio 30 : 70 by weight. After homogenization, the mixture was uniaxially pressed to cylindrical samples (Ø ca. 50 mm, height ca. 10 mm) at 50 MPa (press type ES, Rucks Maschinenbau GmbH/DE). This was followed by a thermal treatment at 1100 °C, simulating the potential application temperature of the synthesized material. Afterwards, the change of diameter of the samples was observed indicating either shrinkage due to melt formation or expansion due to the formation of solid corrosion products. The test was passed when the diameter change due to such reactions was <2 %.

The samples resulting from the shaping experiments were basically characterized. The bulk density was determined from measuring the sample volume by using a mercury displacement volumeter. The total porosity was calculated from the true density which was measured by He-pycnometry (Accupyc 1330, Micromeretics/DE). Refractoriness under load was investigated in accordance to DIN EN ISO 1893 using a Netzsch hood kiln by applying a load of 0,05 MPa and a heating rate of 5 K/min. Thermal conductivity was measured according to DIN 993-15 (hot-wire parallel method) in a TCT 426 (Netzsch/DE). Cold crushing strength was determined on the base of DIN 1094-5 using a TIRA test 2420 (Franz Wohl & Partner/DE). Finally, shaped material was investigated as heat insulation lining in a 10 week laboratory test according to Schlegel [9], which simulated the alkali load in a cement kiln. Fig. 2 shows schematically the testing installation. The salt mixture used in this test consisted of K_2SO_4, KCl and K_2CO_3 analogously to the corrosion test and was replenished weekly.

3 Results and discussion

3. 1 Hydrothermal routine

Tab. 3 summarizes the phase compositions of the hydrothermally synthesized material. It shows that only the stoichiometries KAS_2 and KAS_6 yielded crystalline reaction products without hydrated components. Furthermore, Tab. 3 presents the results of these materials in the corrosion test. The materials of the stoichiometries KAS_2 and KAS_4 passed the test and showed diameter changes below <2 % due to alkali load. Therefore, these materials were treated at temperatures up to 1200 °C (Tab. 3) to determine dimensional changes under thermal load similar to a potential application in a high temperature process. The application of the hydrothermal treatment as synthesis routine followed by the immediate use in the kiln would have been highly appreciated because hydrothermal processes can be conducted with very high energetic effectiveness [11]. However, both materials showed a shrinkage of more than 2 % which was not acceptable for potential high temperature insulation materials (see DIN EN 1094-2). Therefore, the hydrothermal synthesis routine was not pursued further.

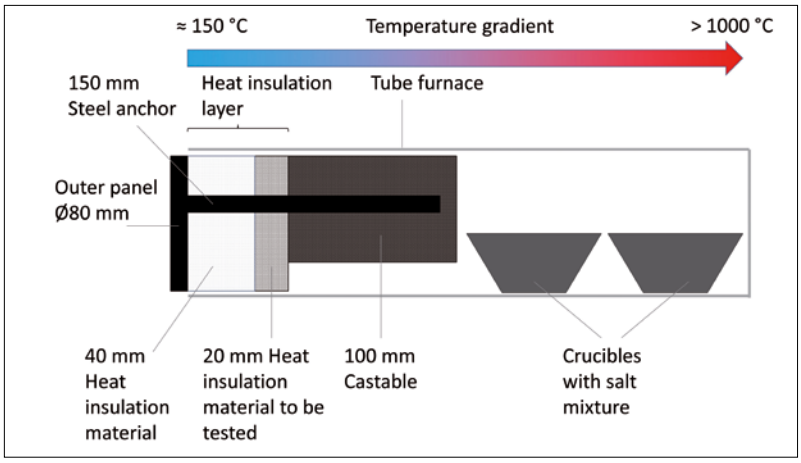

Fig. 2 Schematic draft of the laboratory testing facility according to Schlegel [9]

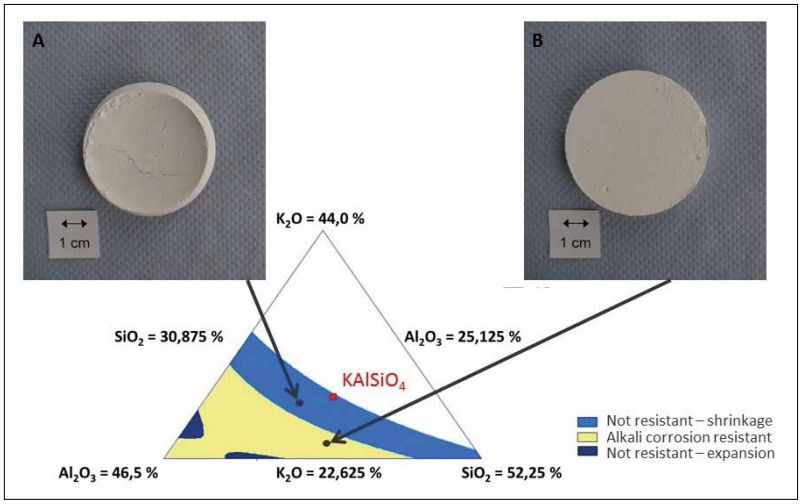

Fig. 3 Compositional regions in the system K_2O–Al_2O_3–SiO_2 (compositions in mass-%) with prediction of their alkali corrosion resistance identified by regression models with two exemplary points A and B, after [12, 13]

3.2 Thermal synthesizing routine

Tab. 4 summarizes the phase analysis of the materials synthesized by the thermal routine [8, 10]. It includes trends of the quantitative evolution of the crystalline phases which was determined by peak height analysis of the main phases. The thermal synthesis routine yielded the intended tar-

Tab. 3 Qualitative phase analysis of the synthesized materials of the hydrothermal routine, their results in the corrosion test and shrinkage behaviour of selected samples at 1200 °C, after [10]

Target Compound	Crystalline Main Phases	Result in Corrosion Test	Shrinkage [%]
KAS_6	$KAlSiO_4$ (kalsilite), $KAlSi_3O_8$ (microcline), quartz	fail	
KAS_4	$KAlSiO_4$ $1{,}5H_2O$, $K_2Al_2Si_3O_{10}$ $2H_2O$	pass	–8,6
KAS_2	$KAlSiO_4$ (hexagonal), quartz, boehmite	pass	–4,4
NAS_6	quartz, zeolite P2, $NaAlSi_2O_6$ H_2O	fail	
NAS_2	$Na_2Al_2Si_3O_{10}(OH)_2$ $2H_2O$	fail	

Tab. 4 Main phases of the synthesized materials produced by the thermal routine, arrows indicate an increase (↑), decrease (↓) or approximate constancy (→) of the amount of a phase for a certain synthesizing temperature with increasing dwell time, after [10]

Target Compound	800 °C	1000 °C	1200 °C
KAS_6	Quartz (↓), amorphous material	Quartz (↓), $KAlSiO_4$ (hex.) (→)	Leucite (→), $KAlSiO_4$ (orthor.) (↓), K-Zeolite (↓)
KAS_4	Quartz (↓), amorphous material	Quartz (↓), $KAlSiO_4$ (hex.) (→)	Leucite (↑), Quartz (↓), $KAlSiO_4$ (orthor.) (↓)
KAS_2	amorphous material	$KAlSiO_4$ (hex.) (→), potassium aluminosilicates (→)	$KAlSiO_4$ (orthor.) (→), Leucite (→)
NAS_6	Quartz (↓), $NAlSiO_4$ (↑)	Quartz (↓), $NAlSiO_4$ (↓)	–
NAS_2	$NAlSiO_4$ (↑), sodium aluminosilicats (↑), Quartz (↓)	$NAlSiO_4$ (↑), sodium aluminosilicats (↑)	$NAlSiO_4$ (→), sodium aluminosilicats (→)

Tab. 5 Results in the corrosion test of the materials synthesized by the thermal routine, o passing of the corrosion test, x failing of the corrosion test, – test not performed [10]

Temperature [°C]										
Target Compound		800			1000			1200		
	Dwell time [h]	3	15	50	3	15	50	3	15	50
KAS_6		x	x	x	x	o	o	o	o	o
KAS_4		o	o	o	x	x	x	o	o	o
KAS_2		o	o	o	o	o	o	o	o	o
NAS_6		x	x	x	x	x	x	–	–	–
NAS_2		x	x	x	x	x	x	x	x	x

get phases as crystalline phases for some synthesizing parameters. However, the reaction products consisted mainly of mixtures of several phases. Partly, quartz originating from the raw materials was still observed in the synthesis products. At low synthesis temperatures (800 °C, partly 1000 °C) high amounts of disordered structures were present which decreased with increasing synthesizing temperature.

Tab. 5 presents the results of the synthesized materials of the thermal routine in the corrosion test. The NAS-based batches did not yield alkali corrosion resistant material although sodium aluminosilicates formed readily in the materials. In the samples of the stoichiometry NAS_6 a melt formation was observed. This was probably related to the relatively low melting point of NAS_6 at 1118 °C. The NAS_2-based samples reacted strongly with the alkali salts used in the corrosion test and showed a shrinkage up to 14 %. A phase analysis of the corroded samples yielded that the material incorporated potassium in its structures forming a potassium-rich nepheline. This corresponded to the phase diagram of K- and Na-nephelines investigated by Tuttle and Smith [12]. The observed shrinkage was attributed to these reactions.

Concerning the KAS-based batches, the behaviour of the investigated materials was very different. Material based on the stoichiometry KAS_2 was remarkable because it showed alkali corrosion resistance independently on the synthesis parameters and the actual phase composition. Highly disordered material, synthesized at 800 °C was equally corrosion resistant as material containing crystalline material of the intended potassium aluminosilicate phases after a synthesis at higher temperatures. The materials based on KAS_4 and KAS_6 were partly alkali corrosion resistant. These stoichiometries had a very similar phase evolution after the synthesis at 800 °C and 1000 °C. But showed almost the opposite results in the corrosion test.

These results showed that the relation between phase composition and corrosion behaviour under alkali load was very complex for both the NAS-based materials and the KAS-based materials [8, 10]. A direct relation between phase composition and corrosion behaviour was not possible to be made. It was concluded that not the crystalline phases which were present in the material were decisive for the corrosion reactions. But structural relations below the length scale of XRD were proposed to play an important role in the materials' behaviour under alkali load.

3.3 Combined routine

The combined routine consisting of a hydrothermal pre-treatment and a thermal synthesis at 1200 °C was investigated for material based on the stoichiometry KAS_2 because of its positive results in the thermal synthesis routine. The aim of the combined routine was to use the positive effect of the hydrothermal treatment on the formation of a porous structure, which would be favourable for heat insulation applications [11]. In the synthesis experiments both types of kaolin were used which differed in their quartz content. Analogously to the thermal processing routine, kaolin 1 (lower quartz content) yielded alkali corrosion resistant material for the stoichiometry KAS_2. For kaolin 2 (higher quartz content), an adjustment of the batch composition was necessary to produce alkali corrosion resistant material [13, 14]. The difference in the quartz content was considered to be the cause for these observations. Regression models were established to describe the corrosion behaviour of a larger compositional area surrounding the stoichiometric point of KAS_2 in the system K_2O–Al_2O_3–SiO_2 as shown in Fig. 3. Fig. 3 includes exemplarily two points A and B of the investigation with photographs of the resulting samples after the corrosion test. Material A shrank strongly whereas material B showed no dimensional changes under alkali load. The comparison of these samples illustrates the different behaviour of the materials depending on their chemical composition.

3.4 Basic characterization of shaped bodies and industrial trial

Point B in the investigated compositional area was chosen to produce formed samples. It was shown that a processing method according to the production of fireclay

i.e. the addition of pre-sintered material of the same composition to the raw material slurry was a promising way to yield crack free shaped bodies [13]. Basic characterizations of these shaped samples were performed. The material had a total porosity of 70 %. The cold crushing strength reached a value of 0,92 MPa. The thermal conductivity was between 0,181 W · (m · K)$^{-1}$ (room temperature) and 0,313 W · (m · K)$^{-1}$ (approx. 1100 °C). The investigation of refractoriness under load yielded $T_{1\,\%}$ = 1344 °C. With these characteristic properties, the produced material was within the property ranges of conventional high temperature heat insulation materials [15].

Finally, the so produced material was investigated as heat insulation lining in the 10 week laboratory test according to Schlegel [9]. The material passed this long-term test and showed no alterations with regard to its dimensions. Furthermore, the main phase of orthorhombic $KAlSiO_4$ remained on a constant level in spite of the alkali attack. Subsequently, protection shells for steel anchors were produced according to Fig. 4 and mounted in an industrial cement kiln in the heat insulation lining (Fig. 5). This component passed an application test of 10 month in the industrial kiln and showed macroscopically a very good post-mortem state in comparison with other conventional materials. The phase composition showed only minor transformations. Additionally to orthorhombic $KAlSiO_4$ as main phase, leucite was observed in the material after the industrial trial. This was attributed to the long-term thermal load.

4 Conclusion

This study focused on a new material approach for high temperature materials under alkali load. The synthesis experiments started from typical corrosion products of fire clay based heat insulation materials such as potassium aluminosilicates or sodium aluminiosilicates. The results showed that the production of heat insulation materials based on potassium aluminosilicates was possible. After investigating a possible shaping technology, the industrial trial showed that they satisfied the requirements for the application as heat insulation material in a cement kiln with regard to alkali corrosion resistance. They represent an interesting new material with a longer service life time due to their alkali corrosion resistance.

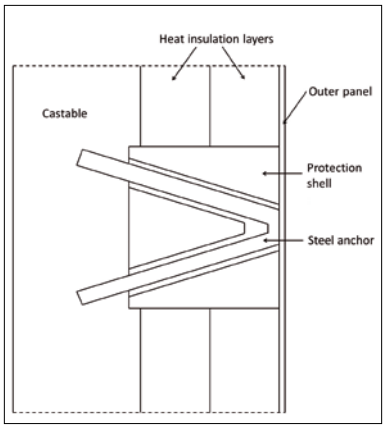

Fig. 4 Schematic draft of the protection shells for steel anchors, after [10]

Fig. 5 Protection shells for steel anchors mounted in an industrial cement kiln [10]

References

[1] Rigby, G.R; Richardson, H.M.: The occurrence of artificial kalsilite and allied potassium aluminum silicates in blast-furnace linings. Min. Mag. **28** (1947) 75–88

[2] Farris, R.E.; Allen, J.E.: Aluminous refractories – alkali reactions. Iron Steel Engin. **50** (1973) 67–74

[3] Schlegel, E.; Fischer, U.; Aneziris, C.G.: Alkali corrosion in cement rotary kilns. InterCeram Manual (2009) 3–8

[4] Brown, J.J.: The use of phase diagrams to predict alkali oxide corrosion of ceramics, in: A.M. Alper (Ed.), Phase diagrams in advanced ceramic, San Diego, CA, 1995, 43–84

[5] Beerkens, R.C.G.; Verheijen, O.S.; Reactions of alkali vapours with silica based refractory in glass furnaces, thermodynamics and mass transfer. Phys. Chem. Glasses **46** (2005) 583–594

[6] Vadasz, P.; et al.: Influence of alternative fuels on the corrosion of basic refractory lining. InterCeram **58** (2009) 130–135

[7] Aneziris, C.G.; Fischer U.; Schlegel, E.: The use of secondary fuels (waste) and the corrosion problems of refractories. Keram. Z. **60** (2008) 347–351

[8] Brachhold, N.; Aneziris, C.G.: Synthesis of alkali aluminosilicates – materials for alkali contaminated environments at high temperatures. Int. J. Appl. Ceram. Technol. **10** (2013) 707–715

[9] Schlegel, E.; Aneziris, C.G.; Fischer, U.: Alkali corrosion of refractory installations in cement kilns – comparison of theory, laboratory tests and practice. Proc. of the 52nd Int. Colloquium on Refractories 2009, Aachen, 60–62

[10] Brachhold, N.: Alkalikorrosionsbeständige Wärmedämmstoffe. PhD Thesis, TU Bergakademie Freiberg 2015

[11] Schlegel, E.: Grundlagen technischer hydrothermaler Prozesse. Freiberger Forschungshefte A655, 12–17, Leipzig 1982

[12] Tuttle, O.F.; Smith, J.V.: The nepheline-kalsilite system: II. phase relations. Amer. J. of Sci. **256** (1958) 571–589

[13] Brachhold, N.; Aneziris. C.G: Porous materials for alkali contaminated environments. J. Europ. Ceram. Soc. **33** (2013) [10] 2013–2021

[14] Brachhold, N.; Schafföner, S.; Aneziris, C.G.: Investigation of alkali corrosion resistance of potassium aluminosilicates using statistical techniques. Ceram. Int., Part **B41** (2015) [1] 1447–1456

[15] Schulle, W.: Feuerfeste Werkstoffe. Feuerfestkeramik; Eigenschaften, prüftechnische Beurteilung, Werkstofftypen. 1st ed. Leipzig 1990